

Experimental Demonstration of Controlled Collective Ion Acceleration with the Ionization-Front Accelerator

C. L. Olson, C. A. Frost, E. L. Patterson, J. P. Anthes, and J. W. Poukey

Sandia National Laboratories, Albuquerque, New Mexico 87185

(Received 25 November 1985)

Experiments with a second-generation collective ion accelerator (IFA-2) are reported. Results demonstrate that ion acceleration with fields of 33 MV/m over 30 cm has been achieved with a controlled collective accelerator for the first time.

PACS numbers: 52.75.Di, 29.15.Dt, 41.80.Dd, 84.70.+p

In collective accelerators,¹⁻³ the collective fields of an ensemble of charged particles are to be used to accelerate a smaller group of charged particles, usually of a different species. In this manner, collective accelerators may produce accelerating fields orders of magnitude higher than those in conventional accelerators. However, the quest for a scalable, working, collective accelerator has proved to be elusive for many years. In the ionization-front accelerator (IFA), the large space-charge field of an intense relativistic electron beam (IREB) is accurately controlled with a laser to produce high-gradient ion acceleration.^{1,4,5} We report here the successful operation of a second-generation collective accelerator system (IFA-2) which demonstrates that particle acceleration with accelerating fields of 33 MV/m over 30 cm has been achieved with a controlled collective accelerator for the first time.

To show that large space-charge fields are possible with an IREB, consider first a long electron beam of uniform density n_e and radius r_b . The beam appears as a rod of charge with peak radial electric field $E_r = 2\pi n_e e r_b$, where e is the charge on an electron. For a steep axial charge-neutralization gradient, the peak axial electric field at the end of the rod of charge is given by $E_z = E_r$,¹ or

$$E_z = 2\pi n_e e r_b. \quad (1)$$

For a modest IREB with energy $\epsilon_e = 1$ MeV, current $I_e = 30$ kA, and $r_b = 1$ cm, we have $n_e = 2.0 \times 10^{12}$ cm⁻³ and $E_z = 180$ MV/m. For higher IREB densities, fields exceeding 1 GV/m will be attainable.⁶ If the IREB is neutralized in a controlled manner, as in the IFA, then these large fields can be used to accelerate charged particles.

In the IFA, controlled neutralization is achieved as shown in Fig. 1. An IREB is injected into a metallic drift tube filled with a low-pressure working gas. The gas pressure is chosen low enough so that the IREB does not significantly ionize it by IREB-induced ionization processes.⁷ Initially the IREB remains stopped and diverges radially because of its own space charge. An ionizing laser beam is then injected through a window along the side of the drift tube. As the laser beam

is swept, it ionizes the working gas, creating a plasma of density $n_p \approx n_e$. The plasma electrons are expelled radially by the IREB space-charge field, leaving a plasma ion background density $n_p^i \approx n_e$ to provide charge neutrality for the IREB. The IREB propagates quickly through the charge-neutralizing plasma region; just ahead of the plasma region the IREB is subjected to its own space-charge field and diverges radially again. The strong potential well associated with the space charge at the head of the IREB follows the moving laser front synchronously. Ions (produced, e.g., by IREB-induced ionization of a light-ion-source gas mixed with the working gas) are trapped in the potential well and experience acceleration as the laser sweep accelerates.

The IFA is a direct extension of the natural collective acceleration process that occurs when an IREB is injected into a low-pressure neutral gas.^{1,8-10} In the natural process the potential well elongates, has a relatively small axial electric field, and moves at constant velocity. In the IFA a steep potential-well back results, with a very high axial electric field, and with a velocity that can be increased by sweeping of the laser.

For a nonrelativistic IFA, the IREB current is chosen with $I_e \leq I_l$ and $v/\gamma \equiv I_e/I_A < 1$ where I_l is the space-charge limiting current^{1,11}

$$I_l = \beta_e (\gamma_e - 1) (mc^3/e) [1 + \ln(R/r_b)]^{-1}, \quad (2)$$

and I_A is the Alfvén-Lawson magnetic stopping current^{1,12,13}

$$I_A = \beta_e \gamma_e mc^3/e. \quad (3)$$

Here $\beta_e c$ is the electron velocity, c is the velocity of light, $\gamma_e = (1 - \beta_e^2)^{-1/2}$, m is the mass of an electron,

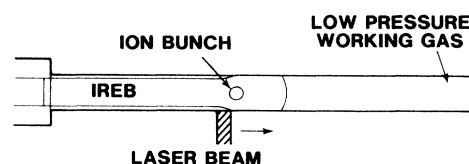


FIG. 1. Ionization-front accelerator (IFA).

and R is the radius of the drift tube. This choice ensures that there is sufficient space charge to create a strong potential well ($I_e \approx I_i$), yet still allow the IREB to propagate easily in the charge-neutralized mode ($I_e < I_A$). The laser is chosen to photoionize the working gas to a plasma density $n_p \approx n_e$ in a time $t \leq \tau$ where $\tau = r_b/\beta_i c$ and $\beta_i c$ is the desired final ion velocity. The IFA concept is very forgiving in that perturbations in γ_e , I_e , or n_p may cause fluctuations in the potential well size but not its axial location. With such perturbations some ions may be lost from the well, but the final energy of the trapped ions will be unchanged because the potential-well axial velocity is determined by the laser sweep velocity.

The energies of the laser, the accelerated ions, and the IREB are ordered respectively as

$$\epsilon_{\text{laser}} \ll \epsilon_{\text{ions}} < \epsilon_{\text{IREB}}. \quad (4)$$

It is emphasized that a very small amount of (expensive) laser photon energy is used to control a very large amount of (inexpensive) pulsed-power IREB energy. The theoretical conversion efficiency of IREB energy into accelerated ion energy should be, e.g., 32% for 300-MeV protons and 10% for 1-GeV protons.¹

Two complete IFA systems have been built (IFA-1 and IFA-2). The first-generation system (IFA-1) had a 10-cm acceleration length and used Cs as the working gas.^{14,15} The second-generation system (IFA-2) has a 30-cm acceleration length,¹⁶ and is shown in Fig. 2. In its final version, IFA-2 uses Cs as the working gas.¹⁷ Three state-of-the-art innovations were created for IFA-2. These are a laser-triggered IREB machine that has nanosecond command firing jitter, a beam-conditioning cell that substantially reduces the IREB current rise time, and an electro-optic crystal deflector that sweeps a high-power laser beam on a nanosecond time scale.

The IFA-2 IREB machine is a pulsed-power driven electron accelerator with laser-triggered Blumlein

switches and a field-emission electron diode. An argon-filled beam-conditioning cell is used to reduce the IREB current rise time from 18 ns to as low as 2.3 ns. The desired IREB parameters at the foil entrance to the IFA acceleration section are 1 MeV, 30 kA, $r_b = 1$ cm, rise time ≤ 5 ns, flat top ≥ 30 ns, and a command firing jitter of ≤ 1 ns. The actual parameters are 1 MeV, 12–42 kA, 3–8 ns rise time, 40 ns FWHM, and a command firing jitter of a few nanoseconds.

The Cs cell contains the main IFA acceleration section. The 30-cm drift tube is a rolled copper screen with an inner radius of 1.1 cm. To obtain the desired neutral Cs density, the Cs cell is placed in an oven heated to about 225°C. A Cs ampule is held at a slightly lower temperature to set the desired reduced gas pressure to about 30 μm , which gives a neutral Cs density of about $1.0 \times 10^{15} \text{ cm}^{-3}$. The IREB density is $n_e \approx 2.0 \times 10^{12} \text{ cm}^{-3}$, and so the Cs has to be ionized only 0.2% to produce $n_p \approx n_e$.

A two-step Cs photoionization scheme is used because the cross section for photoionization of Cs from the excited state is about fifty times larger than the cross section for photoionization from the ground state.^{18,19} A ruby-pumped dye laser (852.1 nm) is spread with a cylindrical lens and used to excite the entire Cs volume. The nominal dye-laser parameters are 100 mJ in a 30-ns pulse. The swept laser beam is produced by an XeCl injection-locked amplifier system (308 nm) that produces a very uniform, very low-divergence beam. The nominal XeCl laser parameters are 1100 mJ, 30–40 ns FWHM, and 75% of the energy into a four-times diffraction-limited spot.

The main portion of the XeCl laser beam is directed into an electro-optic crystal deflector with a $1.1 \times 1.1\text{-cm}^2$ throughput aperture. The deflector contains eleven potassium dideuterium phosphate crystals and produces a maximum deflection angle of 2 mrad for a net 30-kV change in applied potential. Typically, the deflector is biased at -15 kV and an electric driver circuit produces a rise to $+15$ kV with a quadratic temporal dependence. After traversing the optical equivalent of 150 m, the beam sweeps 30 cm along the Cs cell in 20 ns with a quadratic temporal dependence. The sweep time can be changed by change of an inductance in the driver circuit. The desired laser parameters at the Cs cell are 127 mJ in a spot diameter ≤ 2.5 cm. The actual parameters were 65–195 mJ in a spot diameter of about 2.5 cm.

An extensive number of diagnostics were used on the full IFA-2 experiments to monitor the IREB, the Cs working gas, the ion source gas, the dye laser, the XeCl laser, the deflector, the timing, the IREB beam-front motion, and the ion output. Here we will summarize the key photoionization experiment results, and the key ion results from the full IFA-2 experi-

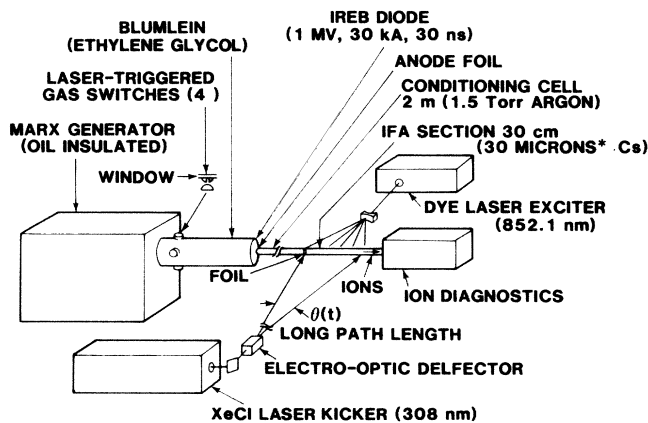


FIG. 2. The IFA-2 system.

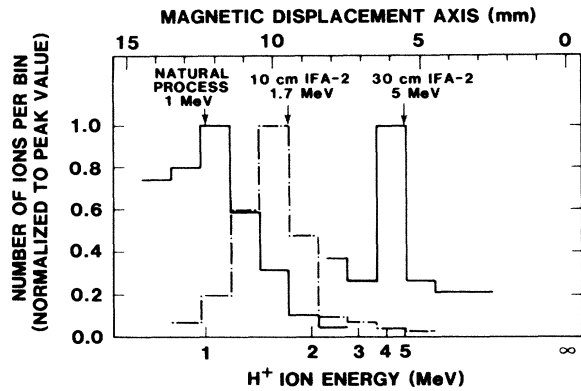


FIG. 3. Proton results.

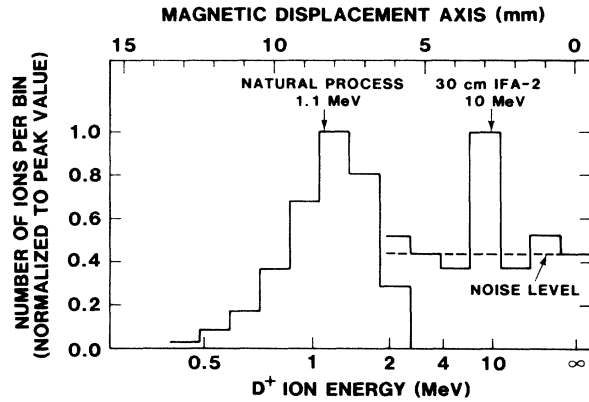


FIG. 4. Deuteron results.

ments.²⁰

Initial experiments were performed to verify that the two-step photoionization scheme was working as planned. In these experiments, the two lasers were used to excite and photoionize the Cs in the first 10 cm of the cell, just before the IREB was injected. Then, by observing with a streak camera whether the IREB stopped at the entrance foil or jumped quickly through the first 10 cm, we were able to observe the threshold for charge neutralization. From these experiments we found, in agreement with theory, that only 0.001 J/cm^2 of dye laser and 0.0005 J/cm^2 of XeCl laser are needed to control 1000 J of IREB energy. These results demonstrate that the photoionization scheme works and that relation (4) holds well.

The main ion results were obtained with a magnetic ion spectrometer using a solid-state nuclear track detector (CR-39). After development of the CR-39 in NaOH, individual ion tracks are produced which may be counted with the aid of a microscope. By division of the CR-39 surface into a series of bins, and counting of the ion tracks in each bin, an energy spectrum can be obtained. In the following, we have normalized each energy spectrum to its peak value, so that energy spectra for different cases may be easily compared.

Proton results are shown in Fig. 3. For the natural collective acceleration process with $100 \mu\text{m}$ H_2 and no lasers, the proton energy peaks at about 1 MeV. For the full IFA-2 system with a 10-cm sweep, and with $50 \mu\text{m}$ Cs and $50 \mu\text{m}$ H_2 , the final velocity β_{1c} was programmed to be $\beta_i = 0.058$ which corresponds to a 1.7-MeV proton. The resultant proton energy spectrum peaks at 1.7 MeV. For the full IFA-2 system with a 30-cm sweep, the final velocity β_{1c} was programmed to be $\beta_i = 0.1$ which corresponds to a 5-MeV proton. The resultant proton energy spectrum peaks at 5 MeV. Deuteron results are given in Fig. 4. Here the natural process for $100 \mu\text{m}$ D_2 produces a D^+ energy peak at about 1 MeV. For the full 30-cm IFA-2 system, with $50 \mu\text{m}$ Cs and $50 \mu\text{m}$ D_2 , the final sweep speed had $\beta_i = 0.1$ corresponding to a 10-MeV D^+ ion. The

resultant D^+ spectrum shows a peak at 10 MeV. Helium-ion results are shown in Fig. 5. Here the natural process for $100 \mu\text{m}$ He produced a peak in the He^{++} spectrum at about 2 MeV. For the full 30-cm IFA-2 system with $50 \mu\text{m}$ Cs and $50 \mu\text{m}$ He, the final sweep speed had $\beta_i = 0.1$ which corresponds to a 20-MeV He^{++} ion. The resultant He^{++} energy spectrum peaks at 20 MeV.

These ion results show that IFA-2 has trapped and accelerated ions at the programmed phase velocity. The D^+ and He^{++} results show that accelerating fields of 33 MV/m over 30 cm were achieved.

The number of ions N that can be trapped should be about $NZ \approx n_b r_b^3$ where Z is the ion charge state.¹ By the assumption of a normal phase-space distribution²¹ for the ion bunch and by the assumption that the bunch is charge neutral and drifts ballistically, a lower-bound estimate for N can be made based on the number of ions in the phase space accepted by the spectrometer, as given in Table I. If the bunch is not charge neutral, then the number of ions could be much higher than the estimates given in Table I. The 30-cm case results are really in a "test particle regime" since the XeCl laser intensity was marginal and there

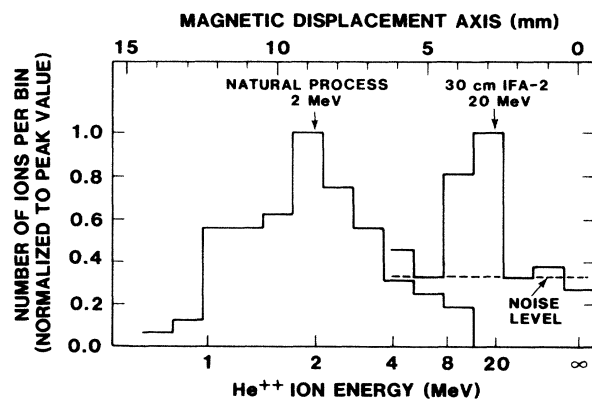


FIG. 5. Helium-ion results.

TABLE I. Lower-bound estimate of N for various cases.

	H ⁺	D ⁺	He ⁺⁺
Natural process	5×10^{12}	1×10^{12}	1×10^{11}
10-cm IFA-2	1×10^{12}
30-cm IFA-2	2×10^{10}	2×10^7	3×10^7

was no opportunity to optimize the laser timing and ion-source gas pressure to maximize N . For the 30-cm case for D⁺ and He⁺⁺, the XeCl laser intensity was about 0.5 MW/cm² at the Cs with a 2.5-cm spot, which yields at the end of the sweep about 0.4 mJ/cm². For the 10-cm case, the XeCl laser intensity was ample (about 0.8 MW/cm² at the Cs with a 1.5-cm spot which yields at the end of the sweep about 0.7 mJ/cm²), and we obtained $N \approx 1.0 \times 10^{12}$. Thus, with proper laser intensity and ion source optimization, we believe $N \geq 10^{12}$ should be routinely attainable for all cases.

As noted with result (1), the IFA-2 IREB is capable of producing a peak E_Z of ~ 180 MV/m. Our present experiment was limited in XeCl laser intensity so that the condition $n_p \approx n_e$ for $\beta_i = 0.1$ was achieved in a distance of about $2.5r_b$ instead of the desired distance $\leq r_b$; this limited the usable field to about 33 MV/m. With proper laser intensity, so that the ionization length is $\leq r_b$, the same experiment should control fields of 100 MV/m over ≥ 1 m.

In conclusion, the physics of the IFA concept has now been demonstrated experimentally. The IFA concept should permit the development of compact accelerators for such diverse fields as nuclear physics, heavy-ion inertial fusion, cancer therapy, and military applications. In addition, the IFA concept can ultimately be extended to the relativistic case ($\beta_i \approx 1$) where the laser pulse is injected on axis and no sweep is needed.⁶ It is then conceivable to have 1-GV/m accelerating fields with 10-m accelerator sections to produce essentially unlimited ion energies.

The assistance of W. Jaramillo and G. Samlin with the experiments is gratefully acknowledged. This work was supported by the Division of Advanced Energy Projects, Department of Energy, and by the Defense Programs, Department of Energy.

¹C. L. Olson and U. Schumacher, *Collective Ion Acceleration*, Springer Tracts in Modern Physics Vol. 84 (Springer-Verlag, Heidelberg, 1979).

²*Collective Methods of Acceleration*, papers presented at the Third International Conference on Collective Methods of Acceleration, edited by N. Rostoker and M. Reiser (Harwood, New York, 1979).

³"Collective Accelerators," report of the U. S. Department of Energy Study Group Report No. FN-355, 1981 (unpublished).

⁴C. L. Olson, in *Proceedings of the Ninth International Conference on High Energy Accelerators*, Stanford Linear Accelerator Center, Stanford, California, 2-7 May 1974 (National Technical Information Service, Springfield, Virginia, 1974), p. 272.

⁵C. L. Olson, in *Proceedings of the International Topical Conference on Electron Beam Research and Technology*, Albuquerque, New Mexico, 3-5 November 1975, edited by Gerold Yonas (National Technical Information Service, Springfield, Virginia, 1976), Vol. 2. p. 312.

⁶C. L. Olson, C. A. Frost, E. L. Patterson, J. P. Anthes, and J. W. Poukey, in *Laser Acceleration of Particles*, edited by C. Joshi and T. Katsouleas, AIP Conference Proceedings No. 130 (American Institute of Physics, New York, 1985), p. 443.

⁷C. L. Olson, Phys. Rev. A **11**, 288 (1975).

⁸C. L. Olson, Phys. Fluids **18**, 585 (1975).

⁹C. L. Olson, Phys. Fluids **18**, 598 (1975).

¹⁰J. W. Poukey and C. L. Olson, Phys. Rev. A **11**, 691 (1975).

¹¹C. L. Olson and J. W. Poukey, Phys. Rev. A **9**, 2631 (1974).

¹²H. Alfvén, Phys. Rev. **55**, 425 (1939).

¹³J. D. Lawson, J. Electron. Control **3**, 587 (1957).

¹⁴C. L. Olson, J. W. Poukey, J. P. VanDevender, A. Owyong, and J. S. Pearlman, IEEE Trans. Nucl. Sci. **24**, 1659 (1977).

¹⁵C. L. Olson, IEEE Trans. Nucl. Sci. **26**, 4231 (1979).

¹⁶C. L. Olson, J. R. Woodworth, C. A. Frost, and R. A. Gerber, IEEE Trans. Nucl. Sci. **28**, 3349 (1981).

¹⁷C. L. Olson, C. A. Frost, E. L. Patterson, and J. W. Poukey, IEEE Trans. Nucl. Sci. **30**, 3189 (1983).

¹⁸K. Y. Nygaard, IEEE J. Quantum Electron. **9**, 1029 (1973).

¹⁹G. V. Marr, *Photoionization Processes in Gases* (Academic, New York, 1967), p. 115.

²⁰A detailed description of the IFA-2 experiments, complete with streak pictures, will be published elsewhere.

²¹A. P. Banford, *The Transport of Charged Particle Beams* (Spon, Ltd., London, 1966), p. 22.